Sequential random close packing of binary disc mixtures

1989 J. Phys.: Condens. Matter 1 2779

(http://iopscience.iop.org/0953-8984/1/17/001)

J. Phys.: Condens. Matter 1 (1989) 2779–2789. Printed in the UK

Sequential random close packing of binary disc mixtures

G C Barker and M J Grimson
Theory and Computational Science Group, AFRC Institute of Food Research, Colney Lane, Norwich NR4 7UA, UK

Received 11 July 1988

Abstract. We present large computer simulations of the sequential random close packing of binary disc mixtures. The growth mechanism is representative of gravity deposition in two dimensions. The details of the composition dependence of the close-packing fraction are related to the form of the structural phase diagram and to the network formed from disc contacts. Limits are placed on the validity of random close-packing models for binary disc mixtures.

1. Introduction

The structures and patterns which are produced by packing discs and disc mixtures in a plane are interesting from many points of view. Random packings made from mixtures of unequal-size discs have been used as models for amorphous and granular materials [1], as examples of systems which contain a controlled amount of disorder and exhibit complex defect structures [2] and as prototype porous media. Close-packed discs are used as the starting point for investigations of size segregation [3], sediment structure [4], trickling flows [5] and sifting phenomena. It is therefore important to establish detailed data concerning the bulk and structural properties of random aggregates formed from hard-disc mixtures. We shall present results, obtained by computer simulation in a strip geometry, for aggregates built by sequential addition of hard discs under the action of a strong unidirectional external force. This growth mechanism is relevant for many experimental configurations involving gravity-controlled deposition.

In [6] experimental non-sequential two-dimensional close packings of binary hard-disc mixtures were constructed and an approximate composition independence found for their average geometrical properties such as the packing fraction and average coordination number. Our computer simulation results for binary hard-disc mixtures show a small systematic dependence of random close-packing fraction c on the ratio $r = R_1/R_2 \leqslant 1$ of disc sizes and the volume fraction x of the smaller discs. Two-dimensional arrays of hard-disc mixtures generated sequentially and deterministically from a seed cluster [2] have a phase diagram which includes a region of 'hexatic' configurations, i.e. configurations of sixfold-coordinated discs with short-range translational order and long-range orientational order. Similar assemblies constructed using a sequential minimum-energy criterion with discs which interact via a short-range pair potential [7] have a very complex phase diagram which also includes regions which correspond to

0953-8984/89/172779 + 11 $02.50

sixfold-coordinated discs. In contrast, the results which we shall present for aggregates built, using a local minimisation of potential energy, under the influence of a unidirectional external field are dominated by fourfold-coordinated configurations.

Disordered packings of hard discs in a plane present a complex theoretical problem in statistical geometry which is most clearly expressed in terms of the network of disc contacts [6]. The network is constructed by connecting the N disc centres by bonds through points of contact between two discs. The average number of contacts per disc is the coordination number z. If the aggregation of discs is stable, as is the case for packings constructed under the action of an external field, each disc has at least two contacts and the contact network is fully connected so that it forms a set of polygons which fill the space. (The polygons may be concave.) Polygons with n sides and average area A_n occur with probability p_n. The set p_n, $n \leq N$, is constrained by normalisation and Euler topology so that we can write [8]

$$\begin{aligned} &\sum_n p_n = 1 \qquad (n > 2) \\ &2z - (z-2)\sum_n n p_n = 0. \end{aligned} \tag{1.1}$$

The packing fraction can be written

$$c = 2\pi\langle R^2\rangle \Big/ \left[\left(z - 2 + \frac{2}{N}\right)\sum_n p_n A_n\right]. \tag{1.2}$$

where $\langle R^2\rangle$ is the mean squared radius of the component discs. In addition the network of disc contacts is constrained by its origin as a stable hard-disc packing. The formulation and expression of these extra 'steric' conditions is crucial for further understanding of the hard-disc packings.

2. Two-dimensional random close packing

The statistical properties of random disc packings depend not only on the details of the sample composition but also on the particular method used to form the packing and on the nature of contacts between particles. We wish to represent the slow deposition of hard frictionless particles in the presence of a strong gravitational field and therefore we use an irreversible ballistic particle-cluster aggregation model in which the incoming particles continuously reduce their potential energy along a trajectory made from a series of linear 'free-fall' and circular-arc 'rotation' sections. The adsorption event is completed when the disc reaches a local potential energy minimum. We may imagine smooth coins sliding down an inclined plane to form a disordered packing.

Our investigations have been limited to two dimensions for computational convenience. There has been much theoretical interest in the two-dimensional problem both fundamentally and as a prototype for the study of three-dimensional disordered packings [9]. In addition the two-dimensional analysis is appropriate for experimental configurations such as packed buoyant spheres or coaxially stacked cylinders (see, e.g., [10]).

We have performed sequential packing simulations in a semi-infinite strip of width L which has an impermeable base line at height $h = 0$. Periodic boundary conditions are applied in the horizontal direction. The packing algorithm represents unidirectional

deposition with multiple restructuring. A disc is introduced at $h = \infty$ with a random lateral coordinate and moves parallel to the strip until it makes contact with either the base line or with another disc (the object disc) which is already part of the aggregate. In the first case the disc aggregates at the point of contact. On contact with the aggregate the incident disc remains in contact with the object disc but rotates around it so as to reduce the h-coordinate of its centre. Rotation proceeds until either the incident disc simultaneously contacts a second aggregated disc (forming a three-disc configuration) or it reaches a position where incident and object disc centres are at the same height. From the latter position the incident disc re-enters the free-fall mode along a different path parallel to the strip. Three-disc configurations are either stable, i.e. the lateral coordinate of the incident disc centre lies between the centre coordinates of the two contacted discs, or unstable in which case the second contacted disc becomes the object disc and a new rotation phase begins. In general, there may be any number of free-fall and rotation phases before the incident disc finds a stable aggregation position but, in practice for $r > 0.25$, the active growth region is only a few disc diameters thick. This observation is essential when constructing computer-simulated disc aggregates containing very large numbers of particles.

It is valuable to compare this growth process with a similar one used in [11] (model III) to study multiple restructuring effects in random deposition of monosize discs. The two algorithms diverge at the point, during a rotation phase, at which the centre of the incident disc attains the same height as that of the centre of the object disc. At this point the model III incident particle continues its rotation path until either it aggregates or it contacts a second aggregated disc and then engages further rotation phases. In our approach the incident disc enters a new free-fall phase of its aggregation trajectory. For purely monodisperse discs these two routes result in identical stable aggregated disc configurations. However, for polydisperse discs, where stable configurations with overhanging discs are permissible, different final configurations may result from the two methods. It has previously been recognised in [11] and, for example in [12], that packing simulations performed on digital machines are inherently polydisperse, to the extent that disordered packings are produced even when initialised with a crystalline seed cluster, so that the results of the two algorithms above inevitably correspond to different growth processes.

3. Results and discussion

We shall label binary disc mixtures by coordinate pairs (x, r) and, for a particular mixture, we shall express all lengths in terms of the diameter of the largest disc. It is for this reason that smaller L-values are appropriate for simulations where the mixture has high x-values and small r-values. Our simulations have been performed on a Vax 11/785 computer using pseudo-random numbers generated by a NAG library FORTRAN subroutine. Each simulation was performed M times, $5 \leqslant M \leqslant 60$, using independent sequences of random numbers to provide an estimate of statistical errors. Packing fractions have been estimated from the central 90% of the occupied volume in order to minimise the effect of the hard base and the upper free surface.

For monodisperse particles $(x, 1)$, it was found in [11] that very-large-scale simulations give ambiguous results for the packing fraction. In table 1, we have listed packing fractions obtained at selected points in the (x, r) plane and, in each case, from simulations performed at three different sizes. It is clear that a complex size dependence occurs in a

Table 1. Packing fraction for sequential random close packing of binary disc mixtures in a strip geometry.

x	r	$N = 2 \times 10^4$ $L = 50$ $M = 50$	$N = 10^5$ $L = 160$ $M = 10$	$N = 5 \times 10^5$ $L = 400$ $M = 5$
1.00	1.0	0.8220(60)	0.8190(46)	0.8177(26)
0.99	0.5	0.8177(34)	0.8153(10)	0.8138(5)
0.90	0.9	0.8134(8)	0.8136(2)	0.8135(1)
0.90	0.5	0.8147(8)	0.8153(5)	0.8150(1)
0.70	0.75	0.8122(6)	0.8123(1)	0.8123(1)
0.70	0.5	0.8155(7)	0.8157(2)	0.8155(1)
0.50	0.9	0.8128(6)	0.8129(3)	0.8128(1)
0.50	0.5	0.8143(8)	0.8143(8)	0.8153(2)
0.50	0.375	0.8218(13)	0.8192(5)	0.8202(2)
0.30	0.75	0.8110(5)	0.8109(2)	0.8109(1)
0.30	0.375	0.8167(12)	0.8176(2)	0.8173(1)
0.10	0.9	0.8135(8)	0.8133(1)	0.8133(1)
0.10	0.375	0.8123(9)	0.8126(2)	0.8126(1)
0.01	0.94	0.8221(50)	0.8185(26)	0.8193(12)
0.01	0.5	0.8126(8)	0.8125(2)	0.8124(1)

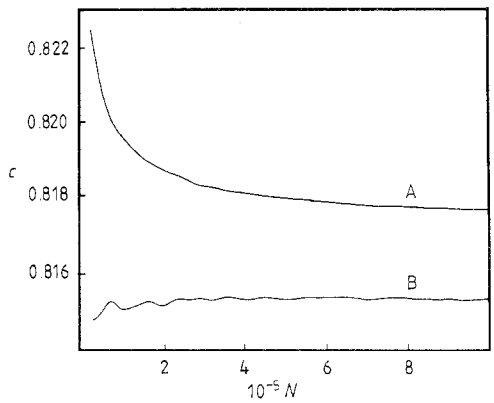

Figure 1. Packing fraction plotted against the number of discs for sequential random close packing: curve A, monosize discs; curve B, binary disc mixture with $x = 0.7$, $r = 0.5$.

small region of the (x, r) plane which is close to the edges of the unit square and also for low-r and high-x mixtures. In the size-dependent region, c is dependent both on system size L and on the number N of particles in the packing. The N dependence of the packing fraction, for $L = 500$ and $N < 10^6$, is illustrated in figure 1 for two of the systems used in table 1. The variation in packing fraction for monosize discs is consistent with that obtained previously in [11] where a slightly different algorithm was used. For $r = 0.5$, $x = 0.7$, the packing fraction is approximately independent of N, for $N > 2 \times 10^4$.

Correlations of the particle positions in a binary disc packing can be measured by the structure function $S(\boldsymbol{q})$ where

$$S(\boldsymbol{q}) = \frac{1}{N}\sum_j \exp(\mathrm{i}\boldsymbol{q} \cdot \boldsymbol{r}_j) \tag{3.1}$$

and $r_j, j = 1, N$, are the positions of the disc centres. We have performed the summations

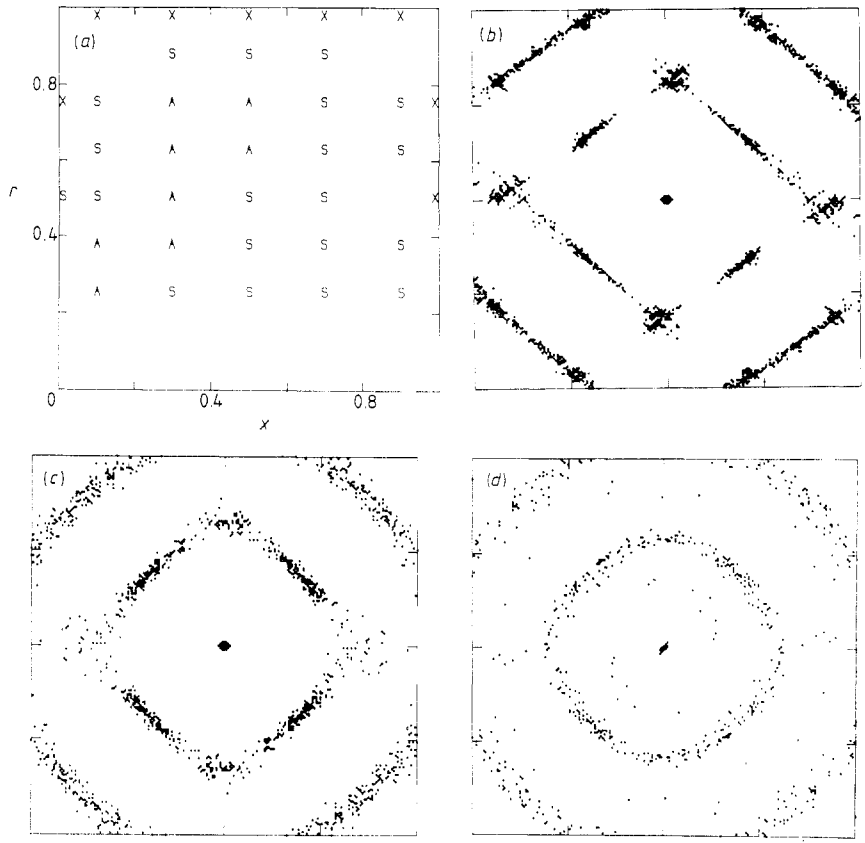

Figure 2. (*a*) Phase diagram for sequential random close packing of binary disc mixtures in a unidirectional external field; (*b*) diffraction pattern for typical X-type configuration; (*c*) diffraction pattern for typical S-type configuration; (*d*) diffraction pattern for typical A-type configuration.

in equation (3.1), over samples of approximately 5×10^3 disc positions extracted from the centre of larger binary disc packings, for an appropriate range of q-values at each of 36 positions in the (x, r) plane. Representative maps of $S(q)$, i.e. diffraction patterns, are constructed by placing a single dot at the end of those $\boldsymbol{q}$-vectors for which $S(\boldsymbol{q})$ is above a threshold value. The results are summarised in figure 2. The phase diagram in figure 2(*a*) can be divided into three regions each characterised by a different set of features in the corresponding diffraction patterns. Three typical patterns, denoted by the letters X, S and A, are illustrated in figures 2(*b*)–2(*d*).

X-type diagrams (figure 2(*b*)) are strongly anisotropic, with approximate twofold symmetry. Diffuse diffraction spots on the axes indicate translational order over a few disc diameters in these directions and their asymmetric displacements indicate that the neighbour distances are larger in the unique direction of the external field. A sharper pattern oriented at 45° to the major axes shows strong translational order in these directions. Although these patterns have features in common with those obtained from crystalline samples, long-range order (which would be apparent from sharp spots in the diffraction pattern) has not been observed in close-packed assemblies of discs formed randomly in an external field.

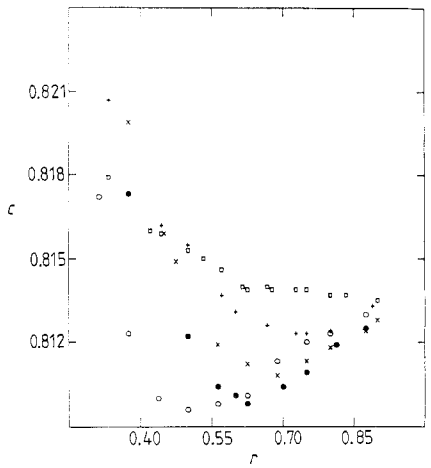

Figure 3. Packing fraction, from computer simulation, plotted against size ratio for sequential random close packing of binary disc mixtures with $x = 0.1$ (○), $x = 0.3$ (●), $x = 0.5$ (×), $x = 0.7$ (+) and $x = 0.9$ (□).

At lower values of r, slightly more disorder is introduced into the disc packings and S-type diffraction patterns (figure 2(*c*)) are produced. The features of S-type patterns are more diffuse, indicating an overall reduction in position correlation, but they remain anisotropic with average fourfold symmetry. Axial correlations are strongly reduced and the patterns at 45° are radially broader than the corresponding features in the X-type patterns. We may conclude that, in these configurations, translational correlations along the (1, 1) directions die out rapidly but that these orientations are always the preferred ones for neighbouring pairs of discs.

Finally A-type patterns are diffuse and isotropic, indicating a total absence of particle correlations other than approximate 'shells' of near neighbours. The corresponding configurations can be considered to be amorphous.

It is difficult to assign a precise meaning to the boundaries which can be drawn between X, S and A regions in figure 2(*a*) but the overall appearance shows a strong resemblance to the phase diagram, given in [2], of binary disc mixtures close packed according to the Bennett algorithm. In both cases a region, at low r, of isotropic disordered configurations is separated from a region in which the configurations show translational and orientational order, i.e. crystalline order, by a region in which orientation effects dominate. (Note that much of the size disparity between the region of hexatic configurations in [11] and our region of S-type configurations is due to the different labels for the x axis, i.e. number and volume fractions, respectively.) The striking difference between the configurations produced by the two methods, i.e. the predominance of sixfold configurations in [11] and of fourfold configurations here, is due to the unidirectional deposition which we have used. The 'deterministic' nature of the Bennett algorithm leads to a stronger 'crystalline' ordering in the region $r \simeq 1$.

Inspection of table 1 shows that, for the phase points which we have tested, the size dependence of the packing fraction is associated with X-type ordering and with low-r high-x configurations. Therefore we have made a systematic computer simulation study of the packing fraction of close-packed binary disc mixtures whose phase point is in the workable S and A regions in figure 2(*a*). In figure 3, we have plotted packing fraction c against size ratio r for five mixture compositions. Data points have been obtained from simulations with either $L = 60$, $N = 2 \times 10^4$ and $M = 50$ or from $L = 160$, $N = 10^5$ and $M = 10$. Statistical errors are typically about 0.0005.

The data sets for $x = 0.1$–0.7 show well defined minima in the region $0.5 < r < 0.75$ whereas for $x = 0.9$, in the range of r we have considered, c increases monotonically with decreasing r. This behaviour can be understood as follows. At a fixed volume fraction of smaller discs, their number fraction is increased by decreasing the size ratio s. Thus, initially, decreasing r from unity at fixed x leads to increased disorder located at each small disc site and to an increase in the number of such sites. Both effects break up correlations between the larger-disc positions and therefore reduce the packing fraction of the assembly. However, although further decrease in r continues to increase the disorder located at individual impurity sites, for small-r and large-x configurations which contain very large numbers of smaller discs, the build-up in position correlations of the smaller discs offsets the disordering effect of size discrepancy and gives a corresponding increase in the packing fraction. This effect is responsible for the size-dependent effects at small r and large x. This mechanism explains the relative position of the minima in figure 3 and would suggest that, without a transition to the X-type structure, the $x = 0.9$ configurations would show a shallow minimum in packing fraction for $0.8 < r < 1.0$.

For the majority of packings which we have constructed, the packing fraction is significantly smaller than the uniform value, $c = 0.84 \pm 0.02$, proposed in [6], for experimental non-sequential close packings of binary disc mixtures. The smallest value of c which we have obtained, $c = 0.8096 \pm 0.0003$, corresponds to the $(0.1, 0.5)$ phase point.

We note that all the data must coincide on the $r = 1$ axis of figure 3 but, because of the X-type ordering for $0.9 \leqslant r \leqslant 1.0$, we cannot rigorously extrapolate our data. However, it is striking that approximate continuation of the set of points in figure 3 leads to a value $c \simeq 0.815$ on the r axis. This is significantly below the accepted value, $c \simeq 0.82$ (see, e.g., [9]) or the result of very-large-scale simulations in [11]. The largest simulation which we have performed, $N = 10^6$, $L = 500$ and $r = 1$, gave the result $c = 0.8177 \pm 0.0026$.

4. Disc contact network

The contact network may be constructed uniquely from a disc packing by forming lines between the two centres of all pairs of discs which are separated by the sum of their two radii. In the case of computer-simulated packings, this scheme is implemented by defining a small but finite capture radius. Details of the disc packings are contained in the polygon distribution p_n and the area law A_n of the networks but comprehensive statistical analyses of large networks, using either algorithmic methods or image-processing techniques, are very expensive. Here we shall present basic information obtained manually from small networks which, in conjunction with the detailed packing data from large simulations, will form a guide to future processing of large-scale disc contact networks. Typical networks are shown in figure 4. They are not easily assessed in terms of a local defect structure and often display features, such as the recurring 'fan' pattern which appears in figure 4(b), which are characteristic of the formation mechanism of the disc packing and which indicate correlations between different cells. From graphical representations of disc contact networks, which correspond to the central portion (2×10^3 polygons) of random disc packings, we have evaluated the polygon fractions p_n and the number fractions t_3^{ijk} of triangle cells formed by i, j, k type of discs in contact ($i, j, k = 1, 2$).

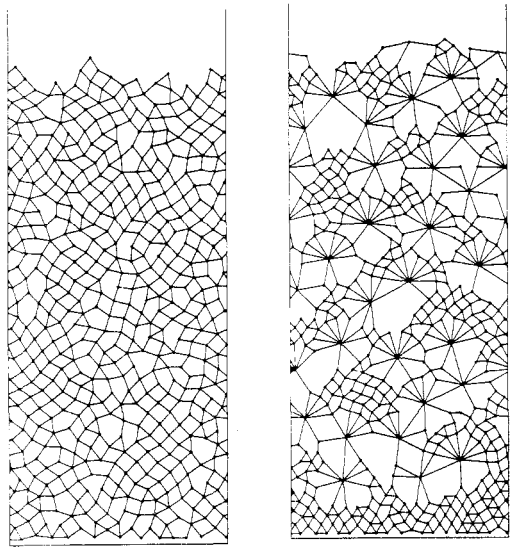

Figure 4. Disc contact networks which correspond to sequential random close packing of binary disc mixtures: (*a*) $x = 0.5$, $r = 0.85$; (*b*) $x = 0.5$, $r = 0.25$.

Within the region of A-type and S-type disc configurations, we have obtained

$$2\sum_n np_n \Big/ \left(\sum_n np_n - 2\right) = z \simeq 4.00 \pm 0.03$$

independent of the composition of the disc mixture. This value is consistent with elementary arguments [13] for counting constraints in two-dimensional packings which contain no short-range order. We shall adopt a constant value $z = 4.0$ in what follows.

Although we have not measured directly the polygon areas A_n we can evaluate A_3 from experimental triangle fractions t_3^{ijk}:

$$A_3/R_2^2 = \sqrt{3}r^2 t_3^{111} + r\sqrt{2r+1}\,t_3^{112} + \sqrt{r(2+r)}\,t_3^{122} + \sqrt{3}t_3^{222}. \tag{4.1}$$

For the contact networks which we have enumerated the fractions t_3^{ijk} are in substantial agreement with weights given by the Dodds statistical geometrical model [14]. The Dodds weights t_n for different n-sided polygons in a contact network, which correspond to a binary disc packing constructed under gravity, are given by the terms of the binomial expansion $(q_1 + q_2)^n$ where

$$q_i = f_i z_i / z \tag{4.2}$$

$$z = f_1 z_1 + f_2 z_2 \tag{4.3}$$

and f_i, z_i are number fractions and component coordination numbers

$$f_1 = 1 - f_2 = 1/[1 + (1-x)r^2/x] \tag{4.4}$$

$$z_1 = 2 + (z-2)r\,/\,(f_2 + f_1 r). \tag{4.5}$$

Average triangle areas calculated using the Dodds weights in equation (4.1) agree with the measured values to within the experimental errors and therefore we adopt this scheme for the polygon fractions because of its semi-quantitative systematic approach.

Many two-dimensional random-network structures exhibit a linear relationship between the average area of a cell and the number of its sides. The empirical statement,

originally for biological tissues only, is Lewis's law (see, e.g. [15]). This result is supported by a maximum-entropy analysis [8] in which the distribution function p_n is chosen to be the most arbitrary one possible subject to the constraints (1.1) and a fixed total area. However, it was observed in [6] that the cell areas obtained from a disc contact network do not follow this simple scheme, i.e. $A_4 > 2A_3$, and, as can be seen from the cell probabilities p_3, p_4, in their table II, the distribution p_n is more complex than the maximum-entropy distribution obtained using a linear-area law for which p_n decreases monotonically with n. The linear-area relationship must therefore be amended to account for unformulated constraints, etc. An extended area law may be written:

$$A_n = A_3(n-2)[1 + (A_4 - 2A_3)(n-3)/2A_3) \tag{4.6}$$

where the second term represents deviations from Lewis's law and is small, about 0.1.

In [6] an expression has been given for the average area of quadrilaterals formed by the centres of four discs in contact (using an assumption of uniformly distributed internal angles) and, although it is unlikely that disc packings constructed under gravity will preserve this angle distribution exactly, we may combine this result with Dodds weights t_4 to estimate A_4. Within this approximation the coefficient $(A_4 - 2A_3)/2A_3$ has a value of 0.1027 for monosize discs and is strongly insensitive to variations in composition for $r > 0.4$ with no deviations greater than 1%. For $r < 0.4$, $(A_4 - 2A_3)/2A_3$ begins to rise sharply.

Rewriting (1.2) using (4.6), we obtain

$$c(x, r) = \pi R_2^2 r^2 / 2A_3[r^2 + x(1-r^2)] \times \left\{1 + (A_4 - 2A_3)(z-2)\left[\left(0.25\sum_n p_n n^2 - 1\right) - 5\right]\Big/ 2A_3\right\}^{-1}. \tag{4.7}$$

The quadratic area law leads to an explicit dependence, on the second moment

$$\sum_n n^2 p_n$$

of the polygon distribution function, for the packing fraction of a random disc packing. Thus the details of the random close packing are associated with the width of the polygon distribution function for the corresponding disc contact network and we can write

$$\sum_n n^2 p_n = [2z/(z-2)]^2 + \sum_n (n - \bar{n})^2 p_n \tag{4.8}$$

where $\bar{n}$ is the mean number of sides per cell. We cannot make a quantitative assessment of equations (4.7) and (4.8). In general, the polygon distribution function of the disc contact network has a small, but finite, width for the random packing of monodisperse discs and becomes broader as impurities are included. Qualitatively, we may write

$$\sum_n p_n (n - \bar{n})^2 = w_0 + w_1 r(1-r) f_1 f_2 \tag{4.9}$$

where w_0 and w_1 are unknown coefficients. Computation of expression (4.7) using equations (4.8) and (4.9) shows that the qualitative features of the packing fraction variations are primarily influenced by the choice of the coefficients w_0 and w_1. In figure 5 we have plotted $c(x, r)$ against r for $x = 0.1, 0.3, 0.5, 0.7, 0.9$, $A_4 - 2A_3 = 0.2054\,A_3$ with $w_0 = 0.1959$ and $w_1 = 5.0$ chosen to give $c(x, 1) = 0.8150$ and $c(0.9, 0.75) = 0.8139$, respectively. The curves in figure 5 show the general features of the packing fraction variations discussed at the end of § 3. Although the precise positions of the

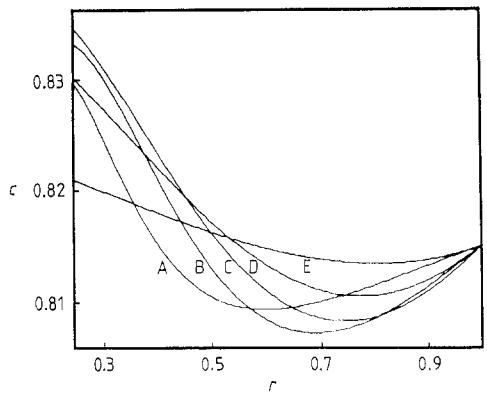

Figure 5. Packing fraction, calculated using a quadratic area law, plotted against size ratio for sequential random close packing of binary disc mixtures with $x = 0.1$ (curve A), $x = 0.3$ (curve B), $x = 0.5$ (curve C), $x = 0.7$ (curve D) and $x = 0.9$ (curve E).

features in figure 5 depend on z, the overall structure is unaltered by variations of z within the range we have measured. If we used the full expression for A_4 [6], the values of c at low r are reduced.

5. Conclusion

The phase diagram for sequential random close packing of binary disc mixtures contains a large central region, where the configurations contain only short-range translational order, in which the packing fraction c falls within a narrow range $0.81 < c < 0.82$. However, by using large computer simulations, in this region we can observe systematic dependence of c on the mixture composition. Significantly the packing fraction is reduced, from the value for sequential random close packing of uniform discs, by the introduction of finite amounts of smaller impurity discs and then rises again as the impurity concentration becomes large. These results indicate the existence of an optimum binary mixture composition which leads to a sequential random close packing which has maximum void space. These variations in the void volume cannot be neglected because the transport and mechanical properties of composite materials strongly depend on the geometrical and compositional heterogeneities [16, 17].

Within the contact network representation of disc packing, the packing fraction behaviour observed above is reproduced by assigning a variable width to the probability distribution function for network polygons. The broadening of this distribution can be seen qualitatively in graphical representations of small networks but, in order to obtain quantitative results for average geometrical properties, it is necessary to use accurate information relating to the second moment

$$\sum_n n^2 p_n$$

which in turn requires the processing of large networks. A small composition dependence of coordination number and deviations from the Dodds statistical model must also be included in a quantitative scheme. The detailed computer simulation results will provide information for assigning the relative significance of these terms. Graphical patterns of the contact network reveal details of local ordering of the two species in binary mixtures. Although this effect has only a small influence on the overall network statistics, and therefore only a small impact on the packing fraction calculations, physical properties of binary disc mixtures, e.g. percolation effects [6, 16], are significantly affected. The

dependence of these correlations on the particular method of construction and on the mixture composition remain open questions.

The phase diagram, for binary disc packings which are built under the influence of a strong unidirectional external field, has a close resemblance to that given in [2], for disc packings constructed using the Bennett algorithm. Although the details of the structures are different, the likeness suggests that the general form of the phase diagram for close packing of binary mixtures of hard discs is largely independent of the particular growth mechanism adopted.

In the region of the phase diagram for which configurations contain significant translational order the packing fraction is dependent on system size. In the extreme case of monosize discs our results confirm those in [11]. We note that, for non-sequential random close packing of hard discs, computer simulations are restricted to system size $N \simeq 10^4$ [18] which is within the size-dependent regime for sequential simulations. Packing fraction results, $c \simeq 0.84$, are significantly higher than those obtained in large sequential simulations.

This approach can be extended to other disc size distributions and the large simulations also provide data concerning surface effects of growth, such as relative sizes of the active growth zones, which will be reported elsewhere. The results that we have obtained direct further research towards the formulation of constraints in terms of the moments of the polygon size distribution of the contact network, which in turn is closely related to the pore size distribution. The simulation results have identified regimes, at the edges of the phase diagram and for $r < 0.25$, in which translational order is a significant feature of the structure in sequentially deposited aggregates.

Acknowledgment

This work was supported by the Ministry of Agriculture, Fisheries and Food.

References

[1] Drescher A and De Josselin de Jong G 1972 *J. Mech. Phys. Solids* **20** 337
[2] Rubinstein M and Nelson D R 1982 *Phys. Rev.* B **26** 6254
[3] Rosato A, Strandburg K J, Prinz F and Swendson R H 1987 *Phys. Rev. Lett.* **58** 1038
[4] Barker G C and Grimson M J 1989 in *Food Colloids* ed. R D Bee, J Mingins and P Richmond (Royal Society of Chemistry) at press
[5] Zimmerman S P and Ng K M 1986 *Chem. Eng. Sci.* **41** 861
[6] Bideau D, Gervois A, Oger L and Troadec J P 1986 *J. Physique* **47** 1697
[7] Livesley D M and Loveday J N 1986 *Phil. Mag.* A **53** 595
[8] Rivier N and Lissowski A 1982 *J. Phys. A: Math. Gen.* **15** L143
[9] Berryman J G 1983 *Phys. Rev.* A **27** 1053
[10] Schneebeli G 1956 *C. R. Acad. Sci., Paris* **243** 125
[11] Meakin P and Jullien R 1987 *J. Physique* **48** 1651
[12] Visscher W M and Bolsterli M 1972 *Nature* **239** 504
[13] Weaire D 1985 *Phil. Mag.* B **51** L19
[14] Dodds J A 1975 *Nature* **256** 187
[15] Weaire D and Rivier N 1984 *Contemp. Phys.* **25** 59
[16] Herrmann H J, Stauffer D and Roux S 1987 *Europhys. Lett.* **3** 265
[17] Travers T, Bideau D, Gervois A, Troudec J P and Messager J C 1986 *J. Phys. A: Math. Gen.* **19** L1033
[18] Jodrey W S and Tory E M 1985 *Phys. Rev.* A **32** 2347